Laser spectroscopy of antiprotonic helium, and the antiproton-to-electron mass ratio measured by ASACUSA

M. HORI
Max-Planck-Institut für Quantenoptik,
Hans-Kopfermann-Strasse 1, D-85748 Garching, Germany

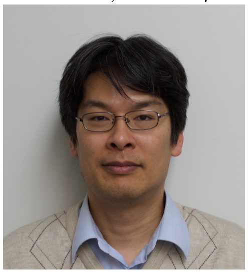

The Atomic Spectroscopy and Collisions Using Slow Antprotons (ASACUSA) collaboration at CERN's Antiproton Decelerator is carrying out laser spectroscopy experiments to measure the atomic transition frequencies of antiprotonic helium ($\overline{p}\mathrm{He}^+$). Techniques such as sub-Doppler two-photon laser spectroscopy and buffer-gas cooling of $\overline{p}\mathrm{He}^+$ to cryogenic temperature $T =$ 1.5–1.7 K are employed to measure the frequencies to a precision of 2.5 parts in 10^9. By comparing the results with three-body quantum electrodynamics calculations, the antiproton-to-electron mass ratio was determined as $M_{\overline{p}}/m_e = 1836.1526734(15)$. This agreed with the known proton-to-electron mass ratio at a precision of 8 parts in 10^{10}.

1 Introduction

Various kinds of hadronic exotic atoms (i.e., atoms in which the orbital electrons are replaced by a π^-, K^-, Σ^-, or $\overline{p}$) have been experimentally studied since the 1950's and 1960's. The energies of the fluorescence X-rays that are emitted when the atoms deexcite between states of low principal quantum number n have been systematically measured with an experimental precision between 10^{-3} and 10^{-6}. These atoms are typically destroyed within picoseconds following formation, as the atom rapidly deexcites to states of low orbital angular momentum quantum number ℓ by undergoing fast electromagnetic cascade processes, before being absorbed into the atomic nucleus. Antiprotonic helium ($\overline{p}\mathrm{He}^+$) is a three-body atom composed of a helium nucleus, an electron in the $1s$ ground state, and an antiproton occupying a Rydberg state of quantum numbers $n \sim \ell - 1 \sim 38$. This atom is unique because it retains a microsecond-scale lifetime against antiproton annihilation in the helium nucleus, even when it is formed in a dense helium target where it collides with other helium atoms at high rates. This is because the electromagnetic cascade processes such as Auger emission of the $1s$ electron and collisional Stark mixing are highly suppressed in $\overline{p}\mathrm{He}^+$ due to its large (25 eV) ionization potential. With the $1s$ electron in place, the antiproton is protected against atomic collisions. The longevity makes $\overline{p}\mathrm{He}^+$ amenable to laser spectroscopic measurements of its transition frequencies with a relative precision of $\sim 10^{-9}$ or better, from which the antiproton-to-electron mass ratio $M_{\overline{p}}/m_e$ can be determined [1,2]. A comparison between the antiproton- and proton-to-electron (M_p/m_e)

mass ratios would constitute a consistency test of CPT symmetry [3,4,5]. In the current system of scientific units [6], M_p/m_e is a dimensionless fundamental constant of nature that can be determined to particularly high precision, as it is the mass ratio between the only stable hadron and charged lepton; laser spectroscopy of $\overline{p}\mathrm{He}^+$ also provides an independent way to determine this constant.

The E1 optical transition frequencies of $\overline{p}\mathrm{He}^+$ have recently been calculated [7,8,9] to a relative precision of $\sim 10^{-10}$ by evaluating the complete set of quantum electrodynamics (QED) corrections up to order $m_e\alpha^7$ in atomic units. These *a priori* calculations used the International Council for Science Committee on Data for Science and Technology (CODATA) 2010 recommended values of the fundamental constants, which include the fine structure constant, the ^{3}He- and ^{4}He-to-electron mass ratios, the Rydberg constant, and the Bohr radius. By comparing these calculated and experimentally-measured $\overline{p}\mathrm{He}^+$ frequencies, $M_{\overline{p}}/m_e$ can in principle be determined to a fractional precision of $< 1\times 10^{-10}$. This may rival the most precise determinations of M_p/m_e in experiments involving a hydrogenic carbon ion $^{12}\mathrm{C}^{5+}$ confined in a Penning trap [10,11,12].

The $\overline{p}\mathrm{He}^+$ can be readily synthesized via the reaction [13], $\overline{p} + \mathrm{He} \rightarrow \overline{p}\mathrm{He}^+ + e^-$, which occurs when a beam of antiprotons are allowed to slow down and come to rest in a helium target. The antiproton is preferentially captured into an orbit with the same radius and binding energy as that of the displaced $1s$ electron. This corresponds to a principle quantum number of $n \sim n_0 = \sqrt{M^*/m_e} = 38$, where M^* denotes the reduced mass of the antiproton–helium nucleus system.

The Atomic Spectroscopy and Collisions Using Slow Antprotons (ASACUSA) collaboration carried out experiments in which laser pulses excited transitions between $\overline{p}\mathrm{He}^+$ states with 1 μs lifetimes, and states that led to Auger emission of the 1s electron within nanosecond lifetimes. The $\overline{p}\mathrm{He}^{2+}$ ion that remained after Auger decay was rapidly destroyed by Stark effects, which mixed the Rydberg ionic states with s, p, and d states at high n during collisions with other helium atoms. This led to antiproton absorption into the helium nucleus within picoseconds. The charged pions that emerged from the annihilation were detected with a Cherenkov detector, thus revealing the resonance condition between the laser and $\overline{p}\mathrm{He}^+$ as a sharp spike in the annihilation rate. ASACUSA has developed various techniques to measure the $\overline{p}\mathrm{He}^+$ frequencies to progressively higher precision.

2 Two-photon laser spectroscopy

In past experiments, the fractional measurement precision of single-photon laser spectroscopy of $\overline{p}\mathrm{He}^+$ was limited to 10^{-7}–10^{-8} by the Doppler broadening effect. As in normal atoms, the thermal motion of $\overline{p}\mathrm{He}^+$ at temperature T strongly broadens the measured width of the laser resonances, by $\nu\sqrt{8k_BT\log 2/Mc^2}$, where ν denotes the transition frequency, k_B the Boltzmann constant, M the atom's mass and c the speed of light. The corresponding loss in spectral resolution limited the precision by which the resonance centroid could be determined.

One way to reach a precision beyond this Doppler limit was provided by two-photon spectroscopy [2]. In the experiment, the $\overline{p}\mathrm{He}^+$ was irradiated by two counterpropagating laser beams, the optical frequencies ν_1 and ν_2 tuned so that their sum $\nu_1 + \nu_2$ corresponded to the $\overline{p}\mathrm{He}^+$ transition frequencies of the type $(n,\ell) \rightarrow (n-2,\ell-2)$. The Doppler shift involving the atom and ν_1 laser was cancelled by the opposite shift relative to the counterpropagating ν_2 laser. To enhance the two-photon transition probability, the laser frequencies were tuned so that the virtual intermediate state of the two-photon transition lay close (within $\Delta\nu_d \approx 10$ GHz) to a real state, $(n-1,\ell-1)$. At resonance between the atom and laser beams, the antiprotons were transferred between the parent and daughter states via the nonlinear transition. The first-order Doppler width was then reduced by a factor $|\nu_1 - \nu_2|/(\nu_1+\nu_2)$, revealing narrow spectral lines.

Three two-photon transition frequencies of $\overline{p}^4\mathrm{He}^+$ and $\overline{p}^3\mathrm{He}^+$ isotopes at ultraviolet wave-

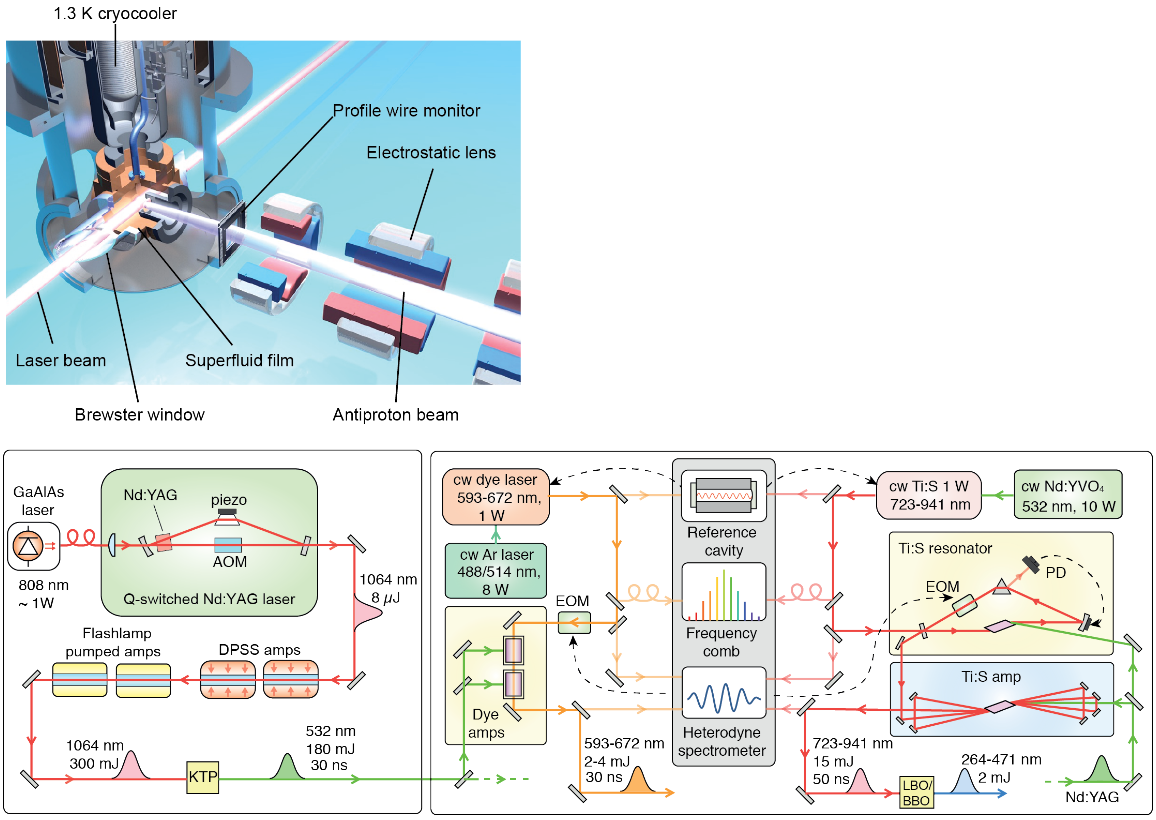

Figure 1 – Schematic drawing [1] of the experimental setup used to synthesize $\overline{p}He^+$ atoms and cooled them to $T = 1.5$–1.7 K (top). Laser system used for laser spectroscopy (bottom).

lengths (λ = 140, 193, and 197 nm) were measured [2] to a precision of 2.3–5 parts in 10^9. The results agreed with the results of three-body QED calculations [7,8] within the experimental uncertainties.

3 Gas-buffer cooling of antiprotonic helium

More recently, ASACUSA cooled some 2×10^9 $\overline{p}He^+$ atoms to a temperature $T = 1.5$–1.7 K by allowing the atoms to undergo elastic collisions with cryogenic helium gas [1]. The density of the buffer helium gas ($T \sim 1.5K$ and $P = 40$–170 Pa) was adjusted so that the $\overline{p}He^+$ atoms, once formed, rapidly underwent a few hundred or more cooling collisions before being interrogated by the laser beam. The 1s electron protected most of the $\overline{p}He^+$ atoms during this cooling.

The experiment (see Fig. 1) was carried out at the Antiproton Decelerator of CERN, which provided a pulsed beam containing 2×10^7 to 3×10^7 antiprotons of kinetic energy $E = 5.3$ MeV and repetition rate 0.01 Hz. About 25% of the antiprotons were decelerated to $E = 75$ keV by allowing them to traverse a 3 m long radiofrequency quadrupole decelerator. The slow antiprotons were then allowed to enter the cryogenic helium gas target in thermal contact with an open-cycle Joule-Thomson cryocooler at $T = 1.3$ K. The $\overline{p}He^+$ thus formed were irradiated by $\Delta t = 40$ to 100 ns long laser pulses with peak powers $P = 0.5$ to 10 kW and wavelengths $\lambda = 264$ to 841 nm.

Figs. 2 (A)–(C) show the profiles of the $\overline{p}{}^4He^+$ transitions $(n, \ell) = (37, 35) \to (38, 34)$, $(39, 35) \to (38, 34)$, and $(38, 35) \to (39, 34)$ obtained by plotting the intensities of the annihilation signals induced at laser frequencies between -1 and 1 GHz around the resonance centroid. In each profile, pairs of fine structure sublines arise from the dominant interaction between the orbital angular momentum of the antiproton and the electron spin. The positions of the four hyperfine sublines that arise from the spin-spin interaction between the antiproton and electron

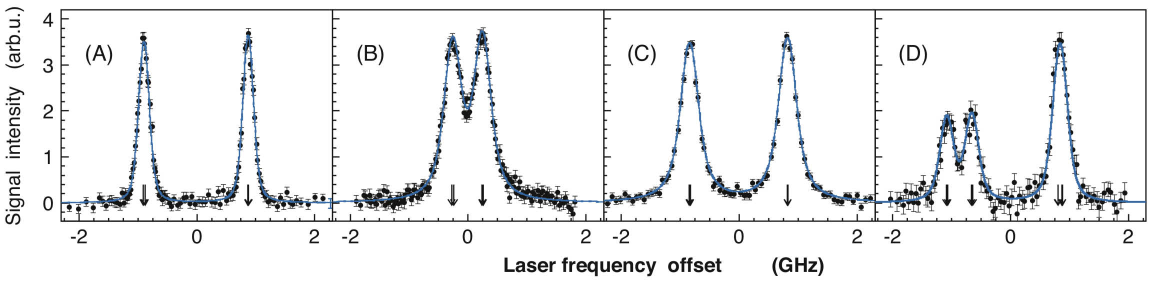

Figure 2 – Resonance profiles of the single-photon transitions (A) $(n, \ell) = (37, 35) \rightarrow (38, 34)$, (B) $(n, \ell) = (39, 35) \rightarrow (38, 34)$, and (C) $(n, \ell) = (38, 35) \rightarrow (39, 34)$ of buffer-gas cooled $\overline{p}^4\mathrm{He}^+$ atoms. (D) The profile $(36, 34) \rightarrow (37, 33)$ of cooled $\overline{p}^3\mathrm{He}^+$ atoms. The x-abscissa indicates the offset of the optical frequency of the laser relative to the resonance centroid. Blue curves indicate best fit of an ab initio model based on the optical Bloch equation.

are indicated in Fig. 2 with arrows. Due to the low $T = 1.5$–1.7 K temperature of the atoms, the single photon resolution seen here exceed those of sub-Doppler two-photon spectroscopy experiments using higher-temperature atoms [2]. Fig. 2 (D) shows the profile of the $\overline{p}^3\mathrm{He}^+$ resonance $(n, \ell) = (36, 34) \rightarrow (37, 33)$. The three-peak structure arises from the eight unequally spaced hyperfine sublines caused by the interactions between the ^{3}He nuclear, electron, and antiproton spins. The spin-independent transition frequencies were determined by fitting the profiles with a theoretical line shape (blue lines), which were obtained by solving the optical Bloch equations.

Some of the experimental uncertainties involved in the determinations of the $\overline{p}\mathrm{He}^+$ frequencies involve the statistical uncertainty (± 1 MHz) arising from the finite number of measured atoms, and a systematic uncertainty of 0.4–3 MHz caused by the fitting function itself. The laser used to excite the atoms contain a spurious frequency modulation which was measured with a precision of 0.4–1.0 MHz. The ac Stark effects and magnetic Zeeman shifts caused systematic effects of order < 0.1 MHz and < 0.2 MHz, respectively.

4 Experimental results

In this way, 13 transition frequencies in $\overline{p}^3\mathrm{He}^+$ and $\overline{p}^4\mathrm{He}^+$ were measured. All the frequencies $\nu_{\rm exp}$ (Fig. 3A, open circles with error bars) agree with theoretical $\nu_{\rm th}$ values (filled squares) within the experimental uncertainties of 2.5×10^{-9} to 15×10^{-9}. This agreement is factor 1.4 to 10 times better than previous single-photon experiments of $\overline{p}\mathrm{He}^+$. The uncertainties for most of the theoretical frequencies $\nu_{\rm th}$ are due to uncalculated QED contributions of orders higher than $m_e\alpha^7$. The corrections of $\nu_{\rm th}$ due to the finite charge radii of the helium nucleus (4 to 7 MHz) and of the antiproton (< 1 MHz) are small because the Rydberg antiproton orbital has negligible overlap with the nucleus and is polarized away from the $1s$ electron.

The calculated frequencies $\nu_{\rm th}$ of the $\overline{p}\mathrm{He}^+$ transitions changed by 2.6×10^{-9} to 2.7×10^{-9} when the antiproton-to-electron mass ratio used in the calculations was changed by 1×10^{-9}. By minimizing the difference between the calculated and experimental frequencies, the mass ratio was determined as,

$$\frac{M_{\overline{p}}}{m_e} = 1836.1526734(15). \tag{1}$$

The one-standard deviation uncertainty in the parenthesis includes the contributions 9×10^{-7}, 11×10^{-7}, and 3×10^{-7} of the experimental statistical and systematic uncertainties, and the theoretical uncertainty, respectively.

The atomic mass of the electron was recently determined [12] with a relative precision of 3×10^{-11} by confining a $^{12}\mathrm{C}^{5+}$ ion in a Penning trap, and measuring the cyclotron frequency of its motion in a magnetic field and the precession frequency of the electron spin. The results were then compared with QED calculations of its g-factor. From this and the known proton

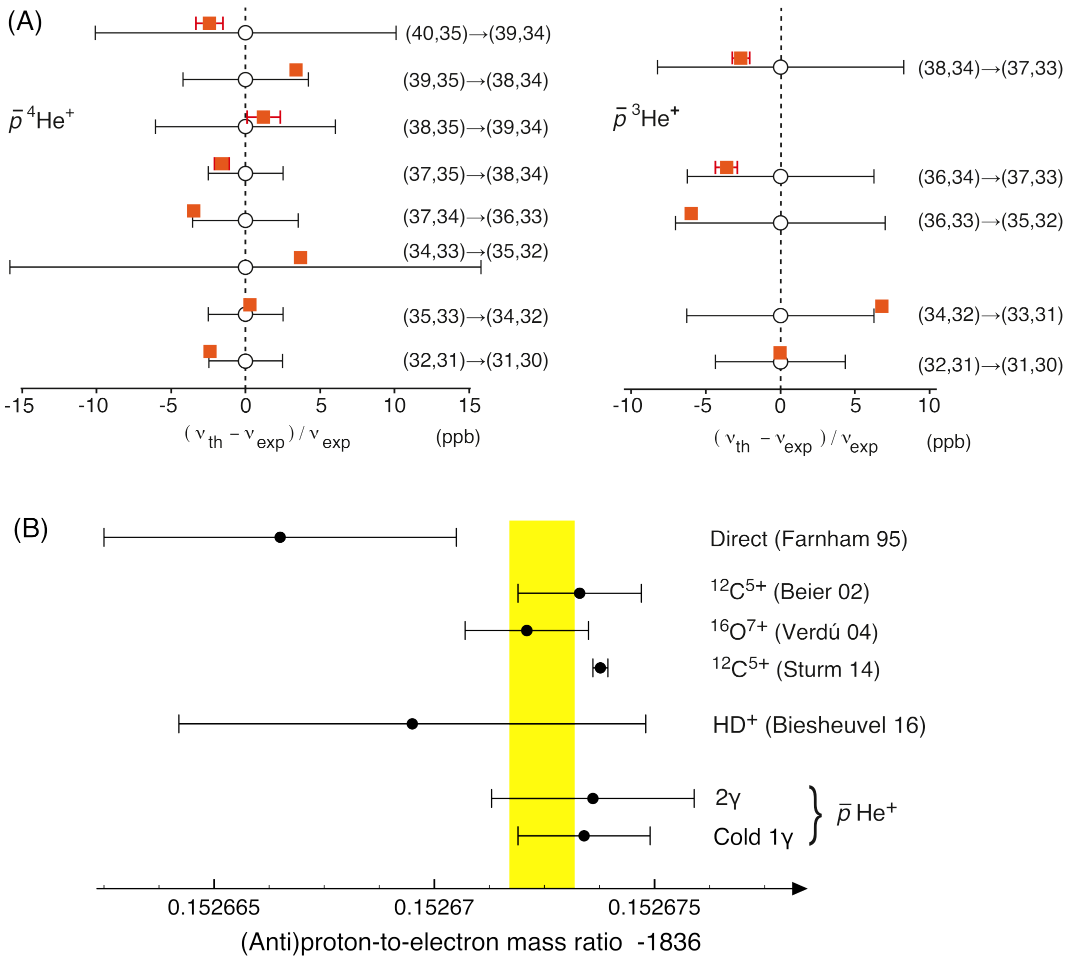

Figure 3 – (A) Comparison of experimental and calculated transition frequencies, showing the fractional differences between the experimental (open circles) and theoretical (squares) values of 13 transition frequencies of cooled $\overline{p}^4\mathrm{He}^+$ and $\overline{p}^3\mathrm{He}^+$ atoms. (B) Proton-to-electron mass ratios measured in Penning traps and laser spectroscopy of HD^+ molecular ions, compared with the antiproton-to-electron mass ratio determined by laser spectroscopy of $\overline{p}\mathrm{He}^+$.

mass, the proton-to-electron mass ratio was determined as,

$$\frac{M_p}{m_e} = 1836.15267377(17). \tag{2}$$

This implies that the proton-to-electron mass ratio is now know with a precision ~ 9 times higher than the antiproton-to-electron value. Fig. 3(B) compares the experimental mass ratios determined by comparing the cyclotron frequencies of protons and electrons in a Penning trap [14], the CODATA recommended value [6], and the ratio determined by means of laser spectroscopy of HD^+ molecular ions [15].

The TRAP and BASE experiments of CERN have compared the cyclotron frequencies of antiprotons and H^- ions confined in a Penning trap [16,17]. By combining the results with the $\overline{p}\mathrm{He}^+$ data of ASACUSA, limits of 5×10^{-10} were set [18,1] on any possible deviation between the antiproton and proton masses and charges.

5 Future developments

The experimental precision of this experiment is now limited by the large emittance, and intensity, position, and energy fluctuations of the antiproton beam provided by the AD which is subsequently decelerated by a radiofrequency quadrupole. CERN is currently constructing the Extra-Low Energy Antiproton Ring (ELENA) facility which provides an antiproton beam of energy 100 keV, the emittance of which is reduced by a factor ~ 100 compared to the current RFQ beam using electron cooling techniques. Using this beam and by incorporating various new lasers, ASACUSA intends to improve the precision of the laser spectroscopy experiments to a precision of $< 1 \times 10^{-10}$. Besides providing a consistency test of CPT symmetry and determining an important fundamental constant $M_{\overline{p}}/m_e$, these experiments also allow tests of QED calculations for three-body systems at the highest levels of precision.

Laser spectroscopy of metastable pionic helium ($\pi\mathrm{He}^+$) is also being attempted at the 590 MeV ring cyclotron facility of the Paul Scherrer Institute. These are three-body atoms [19,20,21] composed of a helium nucleus, an electron occupying the $1s$ ground state, and a negative-charged pion in a Rydberg state of quantum numbers $n \sim \ell - 1 \sim 16$. This experiment may lead to a determination of the charged pion-to-electron mass ratio with a precision of 10^{-8}.

Acknowledgments

I am deeply indebted to the ASACUSA collaboration, the CERN PS and AD operation teams, and to D. Bakalov, T.W. Hänsch, and V.I. Korobov. This research was supported by the Max-Planck Gesellschaft and the European Research Council (ERC-Stg).

References

1. M. Hori, *Science* **354**, 610 (2016).
2. M. Hori, *Nature* **475**, 484 (2011).
3. M. Ahmadi *et al.*, *Nature* **541**, 506 (2017).
4. G. Gabrielse *et al.*, *Phys. Rev. Lett.* **89**, 213401 (2002).
5. S. Aghion *et al.*, *Nat. Commun.* **5**, 4538 (2014).
6. P.J. Mohr, B.N. Taylor, and D.B. Newell, *Rev. Mod. Phys.* **84**, 1527 (2012).
7. V.I. Korobov, L. Hilico, and J.-P. Karr, *Phys. Rev. Lett.* **112**, 103003 (2014).
8. V.I. Korobov, L. Hilico, and J.-P. Karr, *Phys. Rev. A* **89**, 032511 (2014).
9. Mu-Hong Hu *et al.*, *Chem. Phys. Lett.* **654**, 114 (2016).
10. T. Beier *et al.*, *Phys. Rev. Lett.* **88**, 011603 (2002).
11. J. Verdú *et al.*, *Phys. Rev. Lett.* **92**, 093002 (2004).
12. S. Sturm *et al.*, *Nature* **506**, 467 (2014).
13. K. Sakimoto, *Phys. Rev. A* **91**, 042502 (2015).
14. D.L. Farnham, R.S. Van Dyck Jr, and P.D. Schwinberg, *Phys. Rev. Lett.* **75**, 3598 (1995).
15. J. Biesheuvel *et al.* *Nat. Commun.* **7**, 10385 (2016)
16. G. Gabrielse *et al.*, *Phys. Rev. Lett.* **82**, 3198 (1999).
17. S. Ulmer *et al.*, *Nature* **524**, 196 (2015).
18. R.J. Hughes and B.I. Deutch *Phys. Rev. Lett.* **69**, 578 (1992).
19. M. Hori, A. Sótér, and V.I. Korobov, *Phys. Rev. A* **89**, 042515 (2014).
20. V.I. Korobov, A.K. Bakbaev, D.T. Aznabayev, and S.A. Zhaugasheva, *J. Phys. B* **48**, 245006 (2015).
21. B. Obreshkov and D. Bakalov, *Phys. Rev. A* **93**, 062505 (2016).